Geophysical Research Letters

RESEARCH LETTER
10.1029/2020GL092170

Special Section:
The Ice, Cloud and land Elevation Satellite-2 (ICESat-2) on-orbit performance, data discoveries and early science

Space-Borne Cloud-Native Satellite-Derived Bathymetry (SDB) Models Using ICESat-2 And Sentinel-2

N. Thomas[1,2], A. P. Pertiwi[3], D. Traganos[3], D. Lagomasino[4], D. Poursanidis[5], S. Moreno[4], and L. Fatoyinbo[2]

[1]Earth System Science Interdisciplinary Center (ESSIC), University of Maryland, College Park, MD, USA, [2]NASA Goddard Space Flight Center, Biospheric Sciences Laboratory, Greenbelt, MD, USA, [3]German Aerospace Center (DLR), Remote Sensing Technology Institute, Berlin, Germany, [4]Department of Coastal Studies, East Carolina University, Wanchese, NC, USA, [5]Foundation for Research and Technology-Hellas (FORTH), Institute of Applied and Computational Mathematics, The Remote Sensing Lab, Heraklion, Crete, Greece

Abstract Shallow nearshore coastal waters provide a wealth of societal, economic, and ecosystem services, yet their topographic structure is poorly mapped due to a reliance upon expensive and time intensive methods. Space-borne bathymetric mapping has helped address these issues, but has remained largely dependent upon in situ measurements. Here we fuse ICESat-2 lidar data with Sentinel-2 optical imagery, within the Google Earth Engine cloud platform, to create openly available spatially continuous high-resolution bathymetric maps at regional-to-national scales in Florida, Crete and Bermuda. ICESat-2 bathymetric classified photons are used to train three Satellite Derived Bathymetry (SDB) methods, including Lyzenga, Stumpf, and Support Vector Regression algorithms. For each study site the Lyzenga algorithm yielded the lowest RMSE (approx. 10%–15%) when compared with validation data. We demonstrate a means of using ICESat-2 for both model calibration and validation, thus cementing a pathway for fully space-borne estimates of nearshore bathymetry in shallow, clear water environments.

Plain Language Summary Knowledge of the depth of the shallow seafloor in coastal waters is needed for a wide range of applications, including navigation and habitat monitoring. Mapping water depth in these locations is expensive, arduous and sometimes dangerous. To overcome some of these challenges, we used multiple satellite data sets to map water depth in several unique coastal environments. ICESat-2 lidar data is able to sample the depth of the seabed along straight lines in clear water and is then combined with other satellite imagery to derive water depth maps, with acceptable error, containing a level of detail that can exceed some field collected measurements.

Key Points:

- Nearshore bathymetric depths can be retrieved using ICESat-2 lidar data
- ICESat-2 bathymetric data can train Sentinel-2 Satellite Derived Bathymetry (SDB) models at shoreline to island nation scales
- The fusion of ICESat-2 and Sentinel-2 data paves the way for openly available nearshore bathymetry mapping from space

Supporting Information:

- Supporting Information S1

Correspondence to:
N. Thomas and A. P. Pertiwi,
nathan.m.thomas@nasa.gov;
avi.pertiwi@dlr.de

Citation:
Thomas, N., Pertiwi, A. P., Traganos, D., Lagomasino, D., Poursanidis, D., Moreno, S., & Fatoyinbo, L. (2021). Space-borne cloud-native Satellite-Derived Bathymetry (SDB) models using ICESat-2 and Sentinel-2. *Geophysical Research Letters*, *48*, e2020GL092170. https://doi.org/10.1029/2020GL092170

Received 16 DEC 2020
Accepted 27 JAN 2021

1. Introduction

Accurate and current bathymetric maps are essential for coastal management. Emerging demands of the blue economy will open up new opportunities, but have significant impacts on coastal regions and habitats globally (LiVecci et al., 2019). Several key markets that will demand resources from the nearshore environment have been identified for future and continued development including, marine navigation, aquaculture, climate change adaption and mitigation, coastal resilience and disaster recovery. Technological innovation that yields contemporary nearshore seafloor maps with regular repeat observations will enable proper Marine Spatial Planning (MSP) and sharing of coastal waters (Foley et al., 2010; Lester et al., 2016). This is particularly important for Big Ocean States (Small Island Nations) that have limited data access (Flower et al., 2020) or where data does not match local needs (Kelman & West, 2009).

Competing sectors of the Blue Economy will change the bathymetry of nearshore waterways and in a variety of ways. Dredging to meet shipping and navigation demands will increase channel depth and quantity of material spoil (Bishop et al., 2006). Similarly, aquaculture practices such as kelp and oyster farming will reduce erosion and increase sediment accumulation (de Paiva et al., 2018; Zhang et al., 2020). These practices will change the structure of the seafloor and have local-scale implications for sub-aquatic ecosystems and nearshore navigation, by causing rapid changes in benthic morphology. In addition, near-

shore structure is increasingly being looked to as a source of nature-based risk reduction solutions, including the use of natural barriers to sea level rise and storm surges (Spalding et al., 2014). Accurate maps of the seafloor are a critical parameter in measuring the wave attenuation of benthic habitats, like seagrasses and coral reefs (Narayan et al., 2016), and the erosion potential of dune-lined beaches (Schweiger et al., 2020), but up-to-date and repeatable observations of sediment stability and structural complexity are needed (Christianen et al., 2013; Harris et al., 2018). These and other processes are not fully captured by current, openly available bathymetry data (Wolfl et al., 2019), which are limited in spatial and temporal resolution. Increasing this resolution requires financial investment and substantial computation and energy needs to conduct more comprehensive or frequent surveys, particularly to capture the detail required in coastal environments.

There are several free and open initiatives that procure bathymetric data such as the International Hydrographic Organization Data Center for Digital Bathymetry (IHO DCDB; Marks, 2019), European Marine Observation and Data Network (EMODnet; Thierry et al., 2019), the Global Multi-Resolution Topography (GMRT; Ryan et al., 2009) synthesis and the General Bathymetric Chart of the Oceans (GEBCO; Kapoor, 1981). While these initiatives ensure that global bathymetric data are freely available across open oceans, these data are inadequate in shallow waters where the vertical and spatial resolution is insufficient. Singlebeam (SBES) and Multibeam Echo Sounders (MBES) are commonly utilized for local-scale high-resolution mapping (Janowski et al., 2018) but collecting data in shallow water is hazardous and time consuming. Bathymetric lidar data acquired from airborne systems (Kim et al., 2017) circumvent navigation in busy shipping traffic, however they are economically expensive and time-intensive to gather over large areas. Thus existing methods of acquiring bathymetric models face frequent and prohibitive limitations.

Recent advances in Satellite-Derived Bathymetry (SDB) using commercial and open source multispectral Earth Observations have lead to new methodological developments and applications through increased spatial resolution and improved estimations (Caballero and Stumpf, 2020a, 2020b; Casal et al., 2019, 2020; Caballero et al., 2019; Li et al., 2019; Lyons et al., 2020; Mateo-Perez et al., 2020; Poursanidis et al., 2019a; Traganos et al., 2018a). A number of SDB studies have improved water depth retrieval through empirical correlations of surface reflectance with field-acquired depth points (Lyzenga et al., 2006; Stumpf et al., 2003); machine learning that combines surface reflectance and in-situ data (Albright and Glennie, 2020; Geyman and Maloof, 2019; Pan et al., 2015); automatic tuning of SDB to water column conditions (Kerr and Purkis, 2018; Li et al., 2019); tracking surface wave kinematics based on the temporal offset between the satellite's bands (Daly et al., 2020); and physics-based inversion algorithms that produce highly accurate SDB estimations but at the expense of required increased computational power (Casal et al., 2020). Despite the advances in SDB and the recent increased availability of cloud-computing platforms such as the Google Earth Engine and Amazon Web Services, most approaches still rely on airborne/shipborne data and local computing resources.

An ability to widely collect consistent open source SDB calibration and validation data will alleviate some of the limitations in deriving routine nearshore bathymetry. The first release of ICESat-2 data highlighted the potential to acquire global bathymetric lidar data in shallow (<40 m) coastal waters (Markus et al., 2017; Parrish et al., 2019). This exciting new capability is especially timely for coastal ecosystem studies as it paves the way for purely spaceborne SDB approaches in the optically shallow global seascape realm (Albright and Glennie, 2020; Ma et al., 2020). Such fusion approaches between satellite-based multispectral imagery and lidar data are now feasible and could significantly reduce the needed time, costs, and computation to produce seamless SDB maps, especially in data poor regions.

In the present study, we have developed one of the first open source fully space-based approaches to measure nearshore bathymetry in optically shallow waters. The SDBs presented here are derived from a newly designed cloud-native workflow within the Google Earth Engine (GEE) cloud platform (Gorelick et al., 2017) using multi-temporal Sentinel-2 A/B data (Traganos et al., 2018a) and ICESat-2 lidar observations (Parrish et al., 2019). Our primary aim is to evaluate the accuracy, scalability and uncertainties of this approach for retrieving SDB, in comparison to freely available bathymetric Digital Elevation Models (DEMs).

2. Materials and Methods

2.1. Data

2.1.1. ICESat-2

The Ice, Cloud and Elevation Satellite-2 (ICESat-2) is a space-based laser altimeter launched in September 2018. ICESat-2 carries the Advanced Topographic Laser Altimeter System (ATLAS) which is a photon counting lidar, composed of three pairs of beams each separated in the across track direction by 3.3 km, with 90 m between each pair. The pairs of lasers are divided into a strong and a weak beam, based on a 1:4 energy ratio. Each laser has a repetition rate of 10 kHz at a wavelength of 532 nm. Each footprint is separated by 70 cm with a diameter of approximately 13 m. ICESat-2 geolocated photon data is provided in the ATL03 product (Neumann et al., 2020) which is disseminated through the National Snow and Ice Data Center (NSIDC). Detailed instrument specifics can be found in Markus et al., (2017).

2.1.2. Sentinel-2

The estimation of satellite-derived bathymetry is based on Copernicus Sentinel-2 data. Sentinel-2 is a twin-satellite mission with 10-m spatial resolution and a 5-day revisit period, available since June 2015. We utilized both Level-1C (L1C) top-of-atmosphere (TOA) reflectance (23 June 2015 - Present) and Level-2A (L2A) atmospherically corrected surface reflectance (SR, 28 March 201-Present) data sets, available within GEE. The use of L2A data was prioritized, but L1C yielded higher quality at some locations due to increased data availability. L2A and L1C data were not mixed at a single study site. Atmospheric correction was not performed on the L1C data as this is computationally expensive and allows a comparison of the errors between L2A and L1C data.

2.1.3. Ancillary Bathymetric Data

2.1.3.1. NOAA Bathymetry

The Bermuda and Biscayne Bay, Florida topographic-bathymetric Digital Elevation Models (DEMs) were acquired from the NOAA National Centers for Environmental Information using the Bathymetric Data Viewer portal (https://maps.ngdc.noaa.gov/viewers/bathymetry/). The Bermuda DEM, at a resolution of 30–90 m, was collected by multiple institutions over a 20 year period (1993–2012; Sutherland et al., 2013). Data was derived from a variety of measurement techniques including topographic surveys, bathymetric lidar, gridded and raw multibeam bathymetry, and nautical chart sounding depth, that were all combined to create a 30 m DEM. The Biscayne Bay (S200) DEM has a 30 m spatial resolution which was derived from nearly 150,000 soundings collected within the bay from 12 different surveys over a period of 63 years (1930–1993; NOAA, 2018). The data was gridded by prioritizing most recent data and/or highest resolution data. Where data coverage was sparse, generic interpolation and extrapolation models were used to fill gaps. No information on the accuracy of the data sets are disseminated with the data.

2.1.3.2. Singlebeam Sonar

Using low cost fishfinder tools, the collection of bathymetry data at the Gulf of Chania (Crete) was completed June–July 2020 based on the method of Poursanidis et al. (2018), covering a depth range of 2–55 m. Details of the instrument and survey are provided in the supporting information.

2.2. Study Sites

2.2.1. Natura 2000 GR4340003, Crete

The Natura 2000 site GR4340003 is found on the North West of the island of Crete, Greece. The Island bounds the southern border of the Aegean Sea, approximately 160 km south of the Greek mainland, and has an area of 8,336 km^2 and a coastline of 1,413 km. Specifically, the Natura 2000 site GR4340003 "Chersonisos Rodopou – Paralia Maleme – Kolpos Chanion" includes Rodopos peninsula and the coastal area from Kolympari to Platanias, at the NW part of Crete, approximately 20 km from Chania city. The marine part of the site extends to a depth of 50 m and is characterized by the presence of *Posidonia oceanica* seagrass beds and extended reef systems.

2.2.2. Biscayne Bay, Florida

Biscayne Bay is an estuary on the east coast of South Florida (USA) that is ecologically diverse and serves as a nursery for many marine species. The bay is heavily influenced by human activities such as boating, diving, recreational and commercial fishing, and serves as a major shipping port where there are incised channels that can exceed 15 m in depth and require regular dredging. The benthic habitats of the central and southern regions of the bay are dominated by seagrass, which includes *Thalassia testudinum*, with sporadic patch reef complexes (Lirman et al., 2008).

2.2.3. Bermuda

Bermuda is a subtropical Caribbean Island over 1,200 km north of the Bahamas, and 965 km east of North Carolina. It is surrounded by the northernmost coral reef assemblage in the Atlantic Ocean and also includes seagrass beds, mangroves, salt marshes, and rocky and sandy intertidal areas (Coates et al., 2013). The reef complex forms a 2–10 m deep, 1.5 km wide rim that surrounds the northern part of the islands. Patch reefs within the lagoon can be found within 1–2 m of the water surface. Marine transport is important to the island as most resources are imported and shipping channels have been modified to accommodate large cruise ships. Channel dredging has led to water quality issues in nearby regions (Lester et al., 2016).

2.3. Satellite-Derived Bathymetry Modeling

2.3.1. ICESat-2 Bathymetric Photons

ICESat-2 ATL03 data was queried via the Open Altimetry online portal (https://www.openaltimetry.org) where it was subset and downloaded over our regions of interest from the NSIDC server in HDF5 format (Figures 1a, 1b, and 1c). The ATL03 product does not record the true location and elevation of sub-aquatic photons due to the refraction of the laser at the air/water interface and the delayed travel time of the laser through the water column. To correct the offset, accurate longitude, latitude, and photon height corrections were performed using the methods of Parrish et al. (2019). This uses the spacecraft geometry and incident laser refraction at the water surface to correct target photon depths, using inputs that include the ICESat-2 instrument wavelength (532 nm), water salinity (35 Practical Salinity Units (PSU)) at atmospheric pressure and location specific ocean temperatures. Photons were transformed to orthometric height (EGM2008), and local UTM zone. Water surface photons were manually selected using an interactive Python plot and user interpretation The photons located beneath the water surface were then corrected for refraction. Longitude and latitude corrections were minimal and photon depth correction was approximately 25% shallower than the value recorded in the ATL03 data, in line with the calculations of Parrish et al. (2019). Bathymetric photons were isolated from the corrected photons using an interactive Python plot and user interpretation. In areas where no seafloor surface was identified, no bathymetric photons were selected. Examples of the refraction corrected photons and selected bathymetric photons are given in Figures 1g–1i. For each ICESat-2 pass only the high-power beams were utilized. When input into the SDB model, only ICESat-2 depth photons with a system assigned "Land Confidence" level of four were used. This system assigned value is determined by the sensor based upon the detected signal-to-noise ratio and ranges from 0 to 4 from least to most confident. Based on preliminary models, the use of photons with the highest confidence values alone improved the model accuracy. Photons were aggregated into a Sentinel-2 10-m resolution grid where multiple photons within a grid cell were averaged (Figures 1d–1f).

2.3.2. Sentinel-2 Satellite Derived Bathymetry (SDB)

We developed a novel cloud-native geoprocessing workflow to pre-process and synthesize Sentinel-2 data in order to estimate and scale up the SDB models. This new cloud-based workflow builds on the pre-processing and SDB estimation developed by Traganos et al. (2018a) and Traganos et al. (2018b). First, an evolved cloud mask was developed that combines the GEE-based Sentinel-2 Cloud Probability data set, the QA60 band, and metadata information. Next, a multi-temporal mosaic was derived using four Sentinel-2 bands; B1-coastal aerosol (resampled to 10 m), B2-blue, B3-green, and B4-red, as these wavelengths are less susceptible to light attenuation than longer wavelength bands. Based on our work within both temperate and tropical optical conditions (Poursanidis et al., 2019b, 2020), the use of the first four Sentinel-2 bands yields increased accuracies in comparison to the exclusion of one or more bands. This is particularly pertinent to

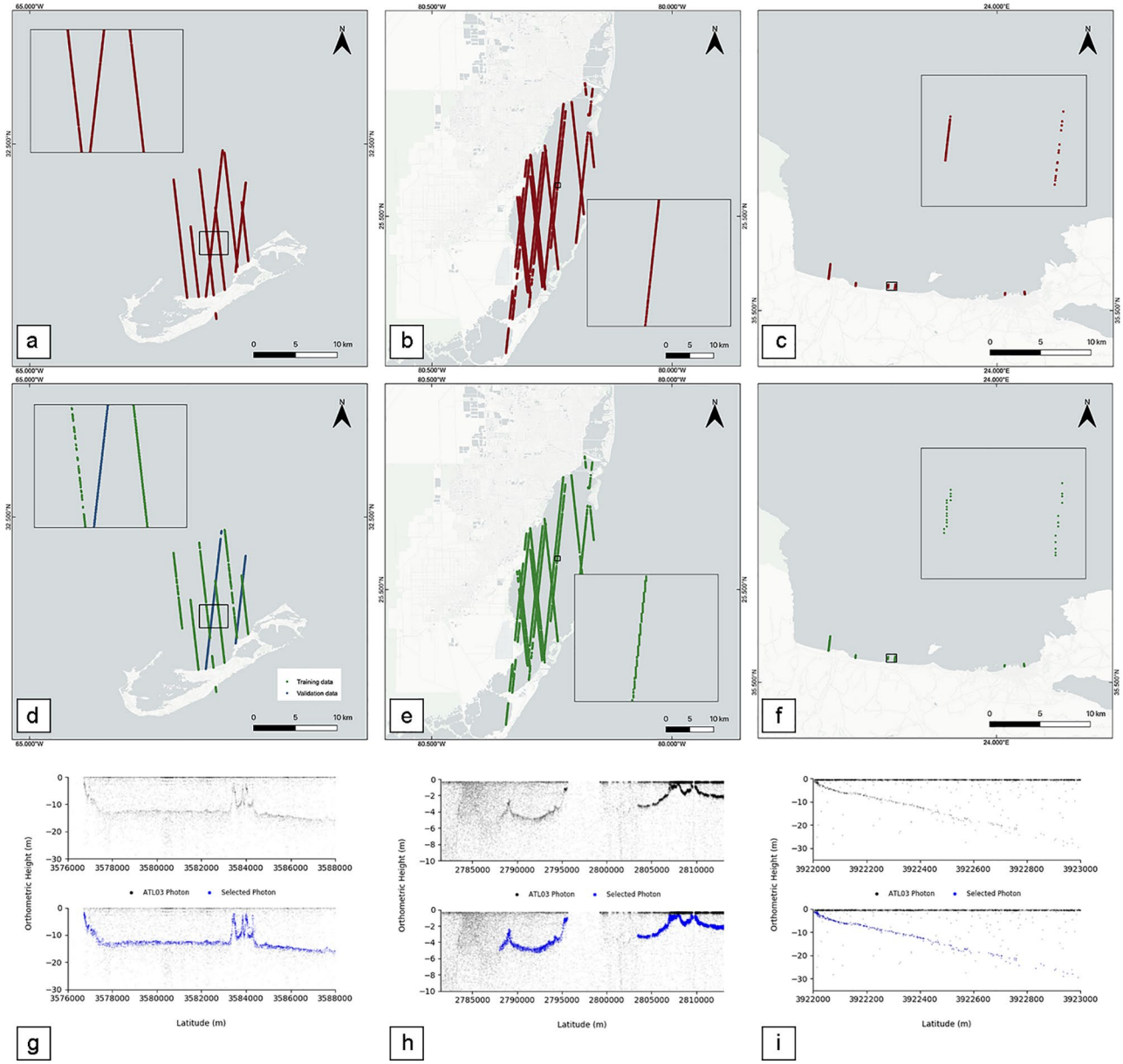

Figure 1. (a, b & c) ICESat-2 depth data points for Bermuda, Biscayne Bay and Crete; (d, e & f) ICESat-2 depth data points with "Land Confidence" level 4 binned to Sentinel-2 10-m resolution for Bermuda (SDB training, green and validation, blue), Biscayne Bay and Crete; (g, h & i) ICESat-2 photons and selected bathymetric profile for a single laser transect in Bermuda, Biscayne Bay and Crete.

the first 5 m of depth within which one can observe the minimum light attenuation in the water column. We derived the mosaic using the twentieth percentile from the cloud masked Sentinel-2 reflectance data cube at each region, which relates to the darker values of the entire reflectance range to ensure the reduction of brighter common natural interferences in satellite images over coastal regions, such as sun glint, turbidity, waves, and remaining clouds and haze.

After the initial pre-processing steps, three cloud-based SDB models were derived using the relationship between the multi-temporal satellite image mosaic and the ICESat-2 data sets. We applied the concept of the cluster-based regression (CBR) algorithm developed by Geyman and Maloof (2019) into two well-known empirical SDB methods: Lyzenga et al. (2006) and Stumpf et al. (2003), in addition to a machine learning Support Vector Regression (SVR). The first method, cluster-based regression with Lyzenga (CBL) algorithm, combined CBR and the log-linear regression SDB method developed by Lyzenga et al. (2006). Prior

Table 1
Root Mean Square Error, Mean Average Error, Standard Deviation, Coefficient of Determination, and Max Depth of the SDB Model Versus Validation Data set in Bermuda, Biscayne Bay, and Crete

Site	Method	RMSE (M)	MAE (M)	μ (M)	σ (M)	R^2	Max depth (M)[a]
Bermuda	CBL	2.62	2.00	0.83	4.48	0.58	26
	CBS	2.89	2.21	0.97	4.03	0.50	26
	SVR	2.96	2.00	0.25	4.89	0.43	26
Biscayne Bay	CBL	0.83	0.65	0.58	0.83	0.72	5
	CBS	1.07	0.90	0.52	0.47	0.30	5
	SVR	0.89	0.73	0.69	0.70	0.64	5
Crete	CBL	2.19	2.02	−0.99	4.99	0.89	22
	CBS	2.41	2.18	−0.7	4.52	0.85	22
	SVR	3.70	2.52	2.6	1.65	0.75	22

[a]based on the ICESat-2 training data sets.

to selecting the relevant bands for modeling, we performed preliminary statistical tests with various combinations of Sentinel-2 bands with this method, and acquired the best accuracy with the multilinear regression of B1, B2, B3, and B4. The second method, cluster-based regression with Stumpf (CBS) algorithm, combined CBR and the log-ratio regression SDB method developed by Stumpf et al. (2003). Our preliminary statistical tests with various cluster-based ratios identified the B3/B2 ratio as the most accurate model (lowest RMSE). The implementation of k-means clustering (Arthur and Vassilvitskii, 2007) prior to the regression in these two methods ensures that by splitting the multi-temporal data into numerous classes, each band adheres to the linear model assumption of homogenous bottom albedo, at each study site. This was particularly beneficial in Bermuda and Biscayne Bay which have variable bottom types. The variable benthic habitats in Bermuda and Biscayne Bay prompted the use of five clusters in the CBL and CBS SDB models. In contrast, Crete features a predominantly homogeneous sandy seabed, averting us from applying clustering prior to the empirical linear and ratio models. In the third method, SVR, we implemented an Epsilon-SVR with the default GEE parameters and a linear kernel to map the first four log-transformed Sentinel-2 bands to a high-dimensional feature space to fit a regression hyperplane. The relationship between ICESat-2 and Sentinel-2 data, for the best performing model, at each study site is presented in Figure S1.

2.4. Reference Data and Accuracy Assessment

We used three different training/validation approaches for each study site which was driven by the availability and quality of reference bathymetric DEM data. Training and validation sample sizes were based on an 80/20 rule with 80% of the sample size used for training and 20% used for validation. For the country of Bermuda, we used six ICESat-2 transects for training (5,173 points) and two ICESat-2 transects for validation–reduced from 2,510 to 1,293 points to fit the 80/20 ratio. Here, the training and validation data were collected on different days, during different passes, which served as separate independent observations. An initial comparison to the NOAA DEM (Bermuda) yielded poor results due to the low temporal and spatial resolution of the DEM (Figures S2 and S3). For Biscayne Bay, ICESat-2 data was used for training (34,342 points) whereas NOAA DEM data was used for validation, using 8,585 (20%) random-stratified points. Lastly, an amalgamation of training with ICESat-2 data (133 points) and with validation data collected from in-situ singlebeam data (85 points) was used in Crete. As a simplifying assumption, for the specific microtidal areas listed, the uncertainty related to data collected at unknown and different-stages of tide was assumed to be small, albeit non-negligible.

For each validation, we calculated the root mean square error (RMSE), mean absolute error (MAE), coefficient of determination (R^2), and the standard deviation of the bathymetry estimation. Residual maps to identify the spatial distribution of the differences between the SDB models and the corresponding NOAA DEMs in Bermuda and Biscayne Bay were also generated (Figures S3 and S4).

3. Results

The CBL method produced the most reliable SDB estimates at all sites with a RMSE of 2.62 m, 0.83 m, and 2.19 m, and MAE of 2 m, 0.65 m, and 2.02 m for Bermuda, Biscayne Bay, and Crete, respectively (Table 1). Among the three methods, SVR tends to underestimate the range of the depths, although its error values do not differ much from that of the CBL method. The RMSEs of the CBL models are lower or close to 10% of the maximum depth for the Bermuda (26 m) and Crete (22 m) models, but close to 17% for the Biscayne Bay model where the maximum depth of the modeled area is much lower (5 m). The R^2 of the models for Bermuda, Biscayne Bay, and Crete were 0.68, 0.79, and 0.83, respectively (Figures 2j–2l). The reference and the modeled depths of Bermuda (Figure 2j) are in good agreement mostly between the depths of 11–17 m, whereas for the shallower Biscayne Bay (Figure 2k) it is between 1.2-3 m.

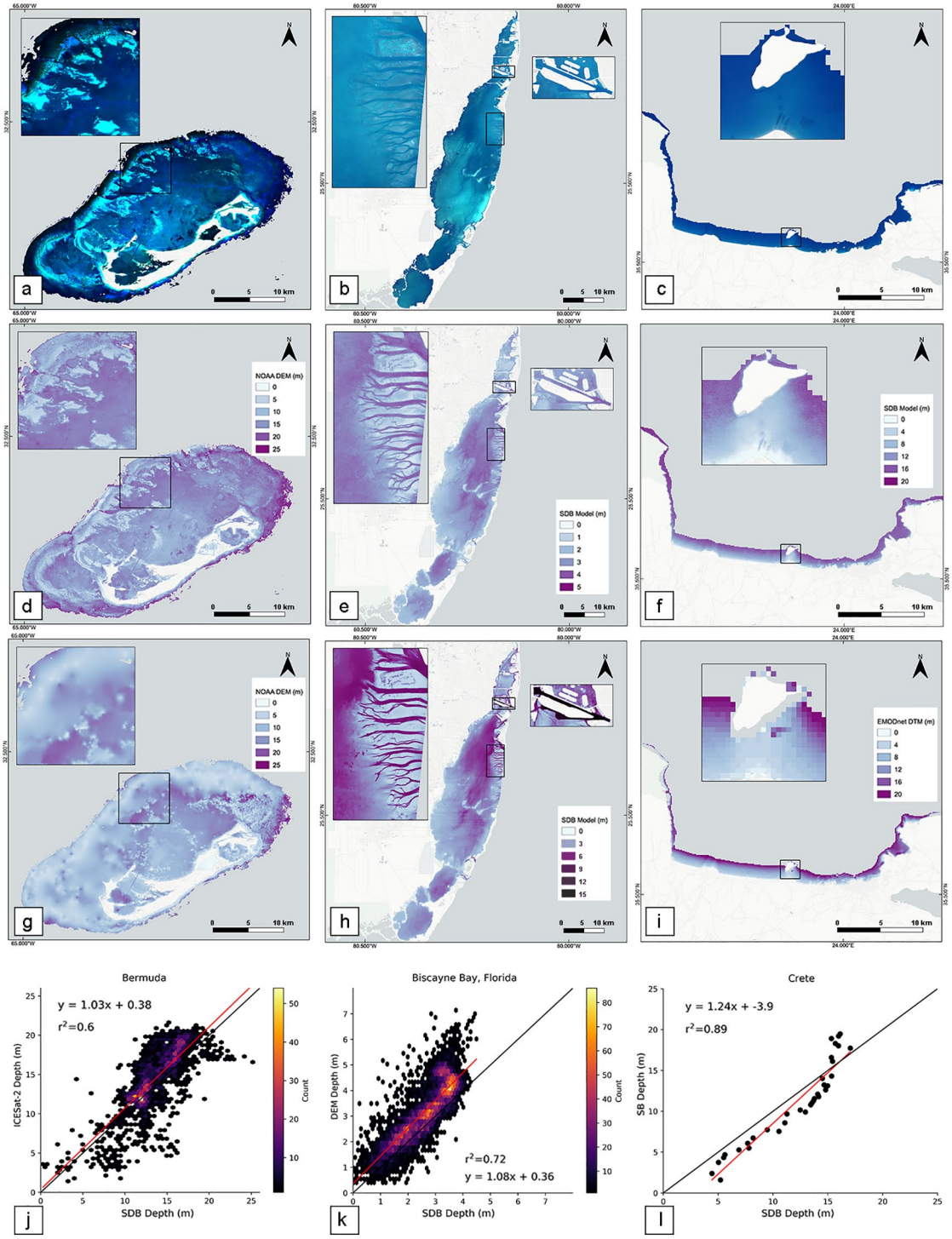

Figure 2. (a, b, c) Sentinel-2 RGB synthesis. (a) Bermuda: 53 L2A Surface Reflectance tiles, 597 km^2 (March 28, 2017 – April 20, 2020); (b) Biscayne Bay: 583 L1C Top-Of-Atmosphere tiles, 689 km^2 (January 1, 2015 – December 31,2019); (c) Crete: L1C 403L1C Top-Of-Atmosphere, 61 km^2 (January 1, 2015 – December 31,2019). (d, e, f) CBL Bathymetry SDB at Bermuda, Biscayne Bay and Crete. (g, h, i) NOAA DEM at Bermuda and Biscayne Bay and EMODnet at Crete, j, k, l) SDB-ICESat-2 depth comparison at Bermuda, Biscayne Bay and Crete.

3.1. Comparison with Publicly Available DEM Data

The detailed Bermuda SDB model picks up the bathymetric relief and rugosity of the shallow and coral reef areas in more detail compared to the NOAA DEM product (Figures 2d and 2g). The Bermuda NOAA DEM product is a merge of multiple data sets and is heavily interpolated in regions with sparse sounding data. In addition the DEM is composed of 63 years worth of data and therefore changes are expected to have occurred due to hurricanes, dredging and other anthropogenic changes (Lester et al., 2016; Smith et al., 2013). For these reasons, we observe high residuals between the Bermuda SDB and NOAA DEM in the coral reef complexes (Figures 2d and 2g). Validation of a preliminary model with the NOAA DEM data yielded a weak ($r^2 = 0.14$) relationship between the NOAA and SDB data, particularly at depths >11 m (Figure S2). The mapped residuals range from −55.96 to 51.28 m, where negative values occur near patch reef complexes and positive values occur within the spur and groove formations of the coral reef rim. The large discrepancy with the NOAA DEM underlined our decision to use ICESat-2 bathymetry photons to validate the SDB DEM at Bermuda.

In Biscayne Bay, the SDB model underestimates the depths of the navigation channels compared to the Biscayne Bay NOAA DEM (Figure 2e and h), particularly within the deep dredged channels around the Port of Miami (Figure 2h) which reach a depth of 17 m. The mapped residuals range from −14.11 to 2.86 m (Figure S4). Photons were able to penetrate the water to these depths, but did not exhibit an obvious surface for training selection.

For the Crete study site, however, the SDB models underpredict the deeper depths, specifically greater than a depth of 15 m, where the water is optically deep. Here the relationship between ICESat-2 reference depths and the log-transformed Sentinel-2 reflectance values become non-linear. The reference and the modeled depths of Crete are in good agreement mostly between the depth of 7–15 m. We obtained an available bathymetric map for the Crete study site for qualitative comparison, but not for validation, from EMODNET, with a resolution of ∼115 m (Figure 2i). Compared to the EMODNET bathymetry map, our Crete SDB model is of much higher spatial resolution (10 m), and features a more gradual change in depth.

4. Discussion and Conclusions

In this study, we have demonstrated the unique fusion of openly available ICESat-2 and Sentinel-2 data for retrieving openly availale shallow water bathymetry DEMs, from coastline to island nation scales. We developed adaptive bathymetry estimation methods derived solely from space-borne observations over coastal waters in Bermuda, Biscayne Bay, and Crete at high-resolution and with low error. The open GEE cloud computing platform provides large computational power and a well-integrated system to process hundreds of multi-temporal images in short time, as well as perform analysis with thousands of data points with ease. The high resolution of Sentinel-2 and ICESat-2 data allows us to map benthic variability in detail, improving upon freely available bathymetry maps, especially within optically shallow water where the reflectance values between different depths are more distinguishable. Errors from L2A and L1C data were comparable, highlighting that computationally expensive atmospheric correction is not needed for accurate SDB retrieval in shallow coastal environments.

Our approach improved upon locally specific and openly available DEM data. Existing DEM data were composed of multiple data sets collected over a large temporal period at varying resolutions. Therefore, changes in seabed structure due to hydrodynamic processes (such as sediment deposition) and natural catastrophes could have been overlooked. At Biscayne Bay, while our RMSE error was small, some uncertainty can be attributed to differences between the high resolution SDB model and lower temporal and spatial resolution NOAA DEM. However, sources of uncertainty are also recognized in the remotely sensed data. At Biscayne Bay, ICESat-2 was unable to detect the bottom of dredged channels, which may have been caused by sediment (turbidity in active shipping lanes) or the inability of the photons to reliably penetrate to those depths. As the ICESat-2 bathymetric photons were manually selected, photons at these depths could be omitted where they did not form a coherent reflecting surface, however the manual selection of photons is simultaneously a potential source of error due to user interpretation. This error may also be present in Bermuda and Crete, particularly where ICESat-2 was used as both training and validation data. Furthermore, a more general source of uncertainty was the effect of tide level in the analysis. By creating Sentinel-2 composite

images using the 20% percentile of tens to hundreds of tiles, we collected the darkest reflectance values, which might not coincide with the depth values acquired by the ICESat-2 platform on a certain acquisition date. The tidal range for our study sites was microtidal (<1 m) thus the advantages of the approach over the small introduction of error are interpreted to be an acceptable tradeoff.

Our SDB models are capable of contributing to the development of the Blue Economy. Without the requirement for in situ data, repeat bathymetric maps can be created for customized time-periods. This flexibility is required for monitoring changes in nearshore topography for the purposes of navigation (Mavraeidopoulos et al., 2017), site assessments, post-disaster mobilization and response (Stronko, 2013), infrastructure developments (Coughlan et al., 2020), and for bathymetry and benthic cover mapping in regions where field data acquisitions are scarce or prevented by a hazardous environment. Coastal zones will experience a future increase in development and impacts from storm events (Horton et al., 2015) and therefore the need for contemporary and repeat bathymetric observations, particularly for data poor regions, will be critical for ensuring sustainability of coastal resources. This is particularly pertinent for "Big Ocean States" (or "Small Island Nations") which may lack the capacity to carry out bathymetric surveys of their territories (Purkis et al., 2019).

Furthermore, our demonstrated method could enable the development of a global map of coastal submerged ecosystems, which continues to be a critical need of the Blue Economy community. This would be the foundation of global habitat accounting for currently poorly mapped sub-aquatic ecosystems as seabed morphology is a usual and helpful parameter in aiding underwater coastal habitat monitoring. Indeed, the need for global distribution maps for seagrasses, a blue carbon ecosystem, has been an issue in coastal ecosystem studies, global conservation efforts and national climate change policy agendas (Unsworth et al., 2019). Moving forward, ensuring vertical reference datum consistency and including tide gauge data or tide models will allow for further characterization of the benthic surface and help to resolve errors across tidal amplitudes. Time series and change detection assessments using pseudo-invariant features could also decrease spectral variabilities in Sentinel-2 composites. We believe that by further characterizing errors and scaling up our approach, we will be able to contribute one of the key factors in making a global map of seagrass, and other shallow benthic habitats, possible.

Data Availability Statement

Data sets are available at: https://doi.org/10.6084/m9.figshare.13017209.v1

Acknowledgments
The authors acknowledge the assistance of Christopher Parrish, Lori Magruder, Amy Neuenschwander, Mike Alonzo and Chrisanthi Praki for their guidance in correcting bathymetric ICESat-2 photons for the effects of refraction. This research was funded by NASA Studies with ICESat-2 Program (Grant No. 80NSSC20K0968). A. Pertiwi and D. Traganos acknowledge funding for their efforts from the German Aerospace Center (DLR) through the Global Seagrass Watch project. Dimitris Poursanidis acknowledges terra Solutions marine environment research for the support in bathymetry data collection for the project "Coastal habitat mapping in support of conservation activities for the loggerhead Caretta caretta" funded by MEDPAN.

References

Albright, A., & Glennie, C. (2020). Nearshore Bathymetry From Fusion of Sentinel-2 and ICESat-2 Observations. *IEEE Geoscience and Remote Sensing Letters*. 1–5. https://doi.org/10.1109/LGRS.2020.2987778

Arthur, D., Vassilvitskii, S., & (2007). k-means++: The advantages of careful seeding, SODA'07. *Proceedings of the eighteenth annual ACM-SIAM symposium on discrete algorithms*, 1027–1035. https://doi.org/10.5555/1283383.1283494

Bishop, M. J., Peterson, C. H., Summerson, H. C., Lenihan, H. S., & Grabowski, J. H. (2006). Deposition and long-shore transport of dredge spoils to nourish beaches: impacts on benthic infauna of an ebb-tidal delta. *Journal of Coastal Research*, *22*(3), 530–546. https://doi.org/10.2112/03-0136.1

Caballero, I., & Stumpf, R. P. (2020a). Atmospheric correction for satellite-derived bathymetry in the Caribbean waters: From a single image to multi-temporal approaches using Sentinel-2A/B. *Optics Express*, *28*(8), 11742–11766. https://doi.org/10.1364/OE.390316

Caballero, I., & Stumpf, R. P. (2020b). Toward routine mapping of shallow bathymetry in environments with variable turbidity: Contribution of Sentinel-2A/B satellites mission. *Remote Sensing*, *12*(3), 451. https://doi.org/10.3390/rs12030451

Caballero, I., Stumpf, R. P., & Meredith, A. (2019). Preliminary assessment of turbidity and chlorophyll impact on bathymetry derived from Sentinel-2A and Sentinel-3A satellites in South Florida. *Remote Sensing*, *11*(6), 645. https://doi.org/10.3390/rs11060645

Casal, G., Harris, P., Monteys, X., Hedley, J., Cahalane, C., & McCarthy, T. (2020). Understanding satellite-derived bathymetry using Sentinel 2 imagery and spatial prediction models. *GIScience and Remote Sensing*, *57*(3), 271–286. https://doi.org/10.1080/15481603.2019.1685198

Casal, G., Hedley, J. D., Monteys, X., Harris, P., Cahalane, C., & McCarthy, T. (2020). *Satellite-derived bathymetry in optically complex waters using a model inversion approach and Sentinel-2 data*, (p. 106814). Estuarine, Coastal and Shelf Science. Retrieved from https://doi.org/10.1016/j.ecss.2020.106814

Christianen, M. J., van Belzen, J., Herman, P. M., van Katwijk, M. M., Lamers, L. P., van Leent, P. J., & Bouma, T. J. (2013). Low-canopy seagrass beds still provide important coastal protection services. *PloS One*, *8*(5). e62413. https://doi.org/10.1371/journal.pone.0062413

Coates, K. A., Fourqurean, J. W., Kenworthy, W. J., Logan, A., Manuel, S. A., & Smith, S. R. (2013). Introduction to Bermuda: geology, oceanography and climate. In *Coral Reefs of the United Kingdom Overseas Territories*. 115–133.Springer. https://doi.org/10.1007/978-94-007-5965-7_10

Coughlan, M., Long, M., & Doherty, P. (2020). Geological and geotechnical constraints in the Irish Sea for offshore renewable energy. *Journal of Maps*, *16*(2), 420–431. https://doi.org/10.1080/17445647.2020.1758811

Daly, C. J., Baba, W., Bergsma, E., Almar, R., & Garlan, T. (2020). *The New Era of Regional Coastal Bathymetry fromSpace: A Showcase for West Africa using Sentinel-2Imagery. Earth ArXiv*, https://doi.org/10.31223/osf.io/f37rv.

de Paiva, J. N. S., Walles, B., Ysebaert, T., & Bouma, T. J. (2018). Understanding the conditionality of ecosystem services: The effect of tidal flat morphology and oyster reef characteristics on sediment stabilization by oyster reefs. *Ecological Engineering*, *112*, 89–95. https://doi.org/10.1016/j.ecoleng.2017.12.020

Foley, M. M., Halpern, B. S., Micheli, F., Armsby, M. H., Caldwell, M. R., Crain, C. M., et al. (2010). Guiding ecological principles for marine spatial planning. *Marine Policy*, *34*(5), 955–966. https://doi.org/10.1016/Fj.marpol.2010.02.001

Flower, J., Ramdeen, R., Estep, A., Thomas, L. R., Francis, S., Goldberg, G., et al. (2020). Marine spatial planning on the Caribbean island of Montserrat: Lessons for data-limited small islands. *Conservation Science and Practice*, *2*(4), e158. https://doi.org/10.1111/csp2.158

Geyman, E. C., & Maloof, A. C. (2019). A simple method for extracting water depth from multispectral satellite imagery in regions of variable bottom type. *Earth and Space Science*, *6*(3), 527–537. https://doi.org/10.1029/2018EA000539

Gorelick, N., Hancher, M., Dixon, M., Ilyushchenko, S., Thau, D., & Moore, R. (2017). Google Earth Engine: Planetary-scale geospatial analysis for everyone. *Remote Sensing of Environment*, *202*, 18–27. https://doi.org/10.1016/j.rse.2017.06.031

Harris, D. L., Rovere, A., Casella, E., Power, H., Canavesio, R., Collin, A., et al. (2018). Coral reef structural complexity provides important coastal protection from waves under rising sea levels. *Science Advances*, *4*(2). eaao4350. https://doi.org/10.1126/sciadv.aao4350

Horton, R., Little, C., Gornitz, V., Bader, D., & Oppenheimer, M. (2015). New York City Panel on Climate Change 2015 report chapter 2: Sea level rise and coastal storms. *Annals of the New York Academy of Sciences*, *1336*(1), 36–44. https://doi.org/10.1111/nyas.12593

Janowski, L., Trzcinska, K., Tegowski, J., Kruss, A., Rucinska-Zjadacz, M., & Pocwiardowski, P. (2018). Nearshore benthic habitat mapping based on multi-frequency, multibeam echosounder data using a combined object-based approach: A case study from the Rowy site in the southern Baltic sea. *Remote Sensing*, *10*(12), 1983. https://doi.org/10.3390/rs10121983

Kapoor, D. C. (1981). General bathymetric chart of the oceans (GEBCO). *Marine Geodesy*, *5*(1), 73–80. https://doi.org/10.1080/15210608109379408

Kelman, I., & West, J. J. (2009). Climate change and small island developing states: a critical review. *Ecological and Environmental Anthropology*, *5*(1), 1–16. https://doi.org/10.1146/annurev-environ-012320-083355

Kerr, J. M., & Purkis, S. (2018). An algorithm for optically-deriving water depth from multispectral imagery in coral reef landscapes in the absence of ground-truth data. *Remote Sensing of Environment*, *210*, 307–324. https://doi.org/10.1016/j.rse.2018.03.024

Kim, H., Lee, S. B., & Min, K. S. (2017). Shoreline change analysis using airborne LiDAR bathymetry for coastal monitoring. *Journal of Coastal Research*, (79), 269–273. https://doi.org/10.2112/SI79-055.1

Lester, S. E., White, C., Mayall, K., & Walter, R. K. (2016). Environmental and economic implications of alternative cruise ship pathways in Bermuda. *Ocean & Coastal Management*, *132*, 70–79. https://doi.org/10.1016/j.ocecoaman.2016.08.015

Li, J., Knapp, D. E., Schill, S. R., Roelfsema, C., Phinn, S., Silman, M., et al. (2019). Adaptive bathymetry estimation for shallow coastal waters using Planet Dove satellites. *Remote Sensing of Environment*, *232*, 111302. https://doi.org/10.1016/j.rse.2019.111302

Lirman, D., Deangelo, G., Serafy, J., Hazra, A., Hazra, D. S., Herlan, J., et al. (2008). Seasonal changes in the abundance and distribution of submerged aquatic vegetation in a highly managed coastal lagoon. *Hydrobiologia*, *596*(1), 105.

LiVecchi, A., Copping, A., Jenne, D., Gorton, A., Preus, R., Gill, G., et al. (2019). *Powering the blue economy; exploring opportunities for marine renewable energy in maritime markets*, p. 207. US Department of Energy, Office of Energy Efficiency and Renewable Energy. Retrieved from https://www.energy.gov/sites/prod/files/2019/03/f61/73355.pdf

Lyons, M., Roelfsema, M., Kennedy, C. V., Kovacs, E. M. E., Borrego-Acevedo, R., Markey, K., et al. (2020). Mapping the world's coral reefs using a global multiscale earth observation framework. *Remote Sensing in Ecology and Conservation*, *6*(4), 557–568. https://doi.org/10.1002/rse2.157

Lyzenga, D. R., Malinaw, N. P., & Tanis, F. J. (2006). Multispectral bathymetry using a simple physically based algorithm. *IEEE Transactions on Geoscience and Remote Sensing*, *44*, 2251–2259. https://doi.org/10.1109/TGRS.2006.872909

Ma, Y., Xu, N., Liu, Z., Yang, B., Yang, F., Wang, X. H., & Li, S. (2020). Satellite-derived bathymetry using the ICESat-2 lidar and Sentinel-2 imagery datasets. *Remote Sensing of Environment*, *250*, 112047. https://doi.org/10.1016/j.rse.2020.112047

Marks, K. (2019). *The IHO-IOC GEBCO cook book*. Retrieved from https://www.gebco.net/data_and_products/gebco_cook_book/

Mateo-Pérez, V., Corral-Bobadilla, M., Ortega-Fernández, F., & Vergara-González, E. P. (2020). Port Bathymetry Mapping Using Support Vector Machine Technique and Sentinel-2 Satellite Imagery. *Remote Sensing*, *12*(13), 2069. https://doi.org/10.3390/rs12132069

Markus, T., Neumann, T., Martino, A., Abdalati, W., Brunt, K., Csatho, B., et al. (2017). The Ice, Cloud, and land Elevation Satellite-2 (ICESat-2): science requirements, concept, and implementation. *Remote Sensing of Environment*, *190*, 260–273. https://doi.org/10.1016/j.rse.2016.12.029

Mavraeidopoulos, A. K., Pallikaris, A., & Oikonomou, E. (2017). Satellite derived bathymetry (SDB) and safety of navigation. *International Hydrographic Review*.

Narayan, S., Beck, M. W., Reguero, B. G., Losada, I. J., Van Wesenbeeck, B., Pontee, N., et al. (2016). The effectiveness, costs and coastal protection benefits of natural and nature-based defences. *PloS One*, *11*(5). e0154735. https://doi.org/10.1371/journal.pone.0154735

National Centers for Environmental Information. (2018). *NOAA NOS Estuarine Bathymetry - Biscayne Bay (S200)*. National Centers for Environmental Information, NOAA. Accessed July 2020. https://doi.org/10.7289/V5GM85N8.

Neumann, T. A., Brenner, A., Hancock, D., Robbins, J., Saba, J., Harbeck, K., et al. (2020). *ATLAS/ICESat-2 L2A global geolocated photon data, version 3*. NASA national Snow and Ice data center distributed active archive center. USA. https://doi.org/10.5067/ATLAS/ATL03.003.

Pan, Z., Glennie, C., Legleiter, C., & Overstreet, B. (2015). Estimation of water depths and turbidity from hyperspectral imagery using support vector regression. *IEEE Geoscience and Remote Sensing Letters*, *12*(10), 2165–2169. https://doi.org/10.1109/LGRS.2015.2453636

Parrish, C. E., Magruder, L. A., Neuenschwander, A. L., Forfinski-Sarkozi, N., Alonzo, M., & Jasinski, M. (2019). Validation of ICESat-2 ATLAS bathymetry and analysis of ATLAS's bathymetric mapping performance. *Remote Sensing*, *11*(14), 1634. https://doi.org/10.3390/rs11141634

Poursanidis, D., Topouzelis, K., & Chrysoulakis, N. (2018). Mapping coastal marine habitats and delineating the deep limits of the Neptune's seagrass meadows using very high resolution Earth observation data. *International Journal of Remote Sensing*, *39*(23), 8670–8687. https://doi.org/10.1080/01431161.2018.1490974

Poursanidis, D., Traganos, D., Chrysoulakis, N., & Reinartz, P. (2019a). Cubesats allow high spatiotemporal estimates of satellite-derived bathymetry. *Remote Sensing*, *11*(11), 1299. https://doi.org/10.3390/rs11111299

Poursanidis, D., Traganos, D., Reinartz, P., & Chrysoulakis, N. (2019b). On the use of Sentinel-2 for coastal habitat mapping and satellite-derived bathymetry estimation using downscaled coastal aerosol band. *International Journal of Applied Earth Observation and Geoinformation*, *80*, 58–70. https://doi.org/10.1016/j.jag.2019.03.012

Poursanidis, D., Traganos, D., Teixeira, L., Shapiro, A., & Muaves, L. (2020) Cloud-native Seascape Mapping of Mozambique's Quirimbas National Park with Sentinel-2. *Remote Sensing in Ecology and Conservation*. https://doi.org/10.1002/rse2.187

Purkis, S. J., Gleason, A. C., Purkis, C. R., Dempsey, A. C., Renaud, P. G., Faisal, M., et al. (2019). High-resolution habitat and bathymetry maps for 65,000 sq. km of Earth's remotest coral reefs. *Coral Reefs*, *38*(3), 467–488. https://doi.org/10.1007/s00338-019-01802-y

Ryan, W. B., Carbotte, S. M., Coplan, J. O., O'Hara, S., Melkonian, A., Arko, R., et al. (2009). Global multi-resolution topography synthesis. *Geochemistry, Geophysics, Geosystems*, *10*(3). https://doi.org/10.1029/2008GC002332

Schweiger, C., Koldrack, N., Kaehler, C., & Schuettrumpf, H. (2020). Influence of Nearshore Bathymetry Changes on the Numerical Modeling of Dune Erosion. *Journal of Coastal Research*, *36*(3), 545–558. https://doi.org/10.2112/JCOASTRES-D-19-00067.1

Smith, S. R., Sarkis, S., Murdoch, T. J., Weil, E., Croquer, A., Bates, N. R., et al. (2013). Threats to coral reefs of Bermuda. In *Coral Reefs of the United Kingdom Overseas Territories*, 173–188. https://doi.org/10.1007/978-94-007-5965-7

Spalding, M. D., Ruffo, S., Lacambra, C., Meliane, I., Hale, L. Z., Shepard, C. C., & Beck, M. W. (2014). The role of ecosystems in coastal protection: Adapting to climate change and coastal hazards. *Ocean & Coastal Management*, *90*, 50–57. https://doi.org/10.1016/j.ocecoaman.2013.09.007

Stronko, J. M. (2013) *Hurricane Sandy Science Plan—Coastal Topographic and Bathymetric Data to Support Hurricane Impact Assessment and Response*, U.S. Geological Survey Fact Sheet. Retrieved from https://pubs.usgs.gov/fs/2013/3099/

Stumpf, R. P., Holderied, K., & Sinclair, M. (2003). Determination of water depth with high-resolution satellite imagery over variable bottom types. *Limnology & Oceanography*, *48*, 547–556. https://doi.org/10.4319/lo.2003.48.1_part_2.0547

Sutherland, M. G., McLean, S. J., Love, M. R., Carignan, K. S., & Eakins, B. W. (2013). Digital Elevation Models of Bermuda: Data Sources, Processing and Analysis 7. NOAA National Geophysical Data Center, US Dept. of Commerce. Retrieved from https://ciresgroups.colorado.edu/coastalDEM/publication/digital-elevation-models-bermuda-data-sources

Thierry, S., Dick, S., George, S., Benoit, L., & Cyrille, P. (2019). June. EMODnet Bathymetry a compilation of bathymetric data in the European waters. In *OCEANS 2019-Marseille* (pp. 1–7). IEEE. https://doi.org/10.1109/OCEANSE.2019.8867250

Traganos, D., Aggarwal, B., Poursanidis, D., Topouzelis, K., Chrysoulakis, N., & Reinartz, P. (2018b). Toward global-scale seagrass mapping and monitoring using Sentinel-2 on Google Earth Engine: The case study of the aegean and ionian seas. *Remote Sensing*, *10*(8), 1227. https://doi.org/10.3390/rs10081227

Traganos, D., Poursanidis, D., Aggarwal, B., Chrysoulakis, N., & Reinartz, P. (2018a). Estimating satellite-derived bathymetry (SDB) with the google earth engine and sentinel-2. *Remote Sensing*, *10*(6), 859. https://doi.org/10.3390/rs10060859

Unsworth, R. K., McKenzie, L. J., Collier, C. J., Cullen-Unsworth, L. C., Duarte, C. M., Eklöf, J. S., et al. (2019). Global challenges for seagrass conservation. *Ambio*, *48*(8), 801–815. https://doi.org/10.1007/s13280-018-1115-y

Wölfl, A. C., Snaith, H., Amirebrahimi, S., Devey, C. W., Dorschel, B., Ferrini, V., et al. (2019). Seafloor Mapping–the challenge of a truly global ocean bathymetry. *Frontiers in Marine Science*, *6*, 283. https://doi.org/10.3389/fmars.2019.00283/full

Zhang, Z., Huang, H., Liu, Y., Bi, H., & Yan, L. (2020). Numerical study of hydrodynamic conditions and sedimentary environments of the suspended kelp aquaculture area in Heini Bay. *Estuarine, Coastal and Shelf Science*, *232*, 106492. https://doi.org/10.1016/j.ecss.2019.106492